Journal of Photochemistry and Photobiology A: Chemistry 346 (2017) 159–167

Contents lists available at ScienceDirect

Journal of Photochemistry and Photobiology A: Chemistry

journal homepage: www.elsevier.com/locate/jphotochem

Photocatalysis effect of a novel green synthesis gadolinium doped titanium dioxide nanoparticles on their biological activities

Shirajahammad M. Hunagund[a], Vani R. Desai[a], Delicia A. Barretto[b], Malatesh S. Pujar[a], Jagadish S. Kadadevarmath[a], Shyamkumar Vootla[b], Ashok H. Sidarai[a,*]

[a] Department of Studies in Physics, Karnatak University, Dharwad-580003, Karnataka, India
[b] Department of Biotechnology and Microbiology, Karnatak University, Dharwad-580003, Karnataka, India

ARTICLE INFO

Article history:
Received 25 March 2017
Received in revised form 1 June 2017
Accepted 2 June 2017
Available online xxx

Keywords:
Antimicrobial
Antioxidant
Gadolinium
Hydrothermal method
Piper betel leaf

ABSTRACT

We report the synthesis of gadolinium doped titanium dioxide (GdT) nanoparticles (NPs) via hydrothermal method using a novel bioreductant *Piper betel* leaf. The physiochemical properties of green synthesized GdT NPs were characterized using various techniques. The results reveal that GdT NPs have attached with the biomolecules which were supporting evidence for the reduction and capping agents. GdT NPs have crystalline in nature and their estimated grain size is of about 5.45 nm by the Scherer's formula. GdT NPs consist of well-dispersed agglomerates of grains with a narrow size distribution of about 4 nm to 7 nm and are having spherical in nature. GdT NPs are thermally stable. In addition, GdT NPs were subjected to antimicrobial and antioxidant assays. Herein, we observed that the GdT NPs show higher antibacterial activities against *Staphylococcus aureus* as compared with *Escherichia coli* and the minimum inhibitory concentration (MIC) value was found to be 25 $\mu g\,mL^{-1}$ under UV irradiation condition for both the cases. Furthermore, antioxidant activities of GdT NPs were evaluated in vitro, using the 1, 1- diphenyl-2-picrylhydrazyl (DPPH) radical cation decolorization test. Results suggest that GdT NPs give promising antioxidant activity as compared to standard ascorbic acid and *Piper betel* leaf. This novel and efficient strategy will show the route for avoiding the use of toxic solvents and a promising green route to restrict for drug discovery from natural products. Thus, the present findings may shine in the field of green pharmaceuticals industries.

1. Introduction

Green chemistry is gaining tremendous importance in the day to day life due to its potentiality of synthesizing materials of various shapes and sizes using naturally occurring bioreductions [1]. There has been growing much interest for the creation of nanoscale materials using the greener route. In recent past, inorganic nanoparticles (NPs) whose structures exhibit significantly novel and improved physical, chemical and biological properties due to their nanoscale sizes have elicited much interest [2–4]. For the NPs, interesting optical, electronic and catalytic effects are expected on the nanoscale [5]. Various approaches are available for the synthesis of NPs [6–12].

In recent times, some attention has been focused on the green route for the synthesis of NPs. The use of environmentally benign plant materials like leaf [13], root [14] and fruit [15] for the synthesis of NPs offers numerous benefits because of their benign nature as well as safety and environmental concerns. The plant extract having the phytochemicals (Tannins, flavonoids and proteins etc.) are the key issue for the controlling the size and shape [1]. Therefore, the presence of stabilizers and various surfactants are desirable to have a control over the growth of the particles.

Titanium dioxide (TiO_2) NPs are well recognized as a versatile multifunctional material due to their superior chemical stability under physiological environment and non-toxicity etc. [16,17]. The TiO_2 material has been widely using in the area of solar cells [18], sensor [19], biological activities [20] and catalyst [21]. In view of these facts, we have chosen TiO_2 material for our study. Several researchers were successfully synthesized TiO_2 nanomaterials using plants leaf [22,23], fruit [24], root [25] and fungus [26] for the biological applications. Some transition elements and some rare earth materials were doped with the TiO_2 material in order to enhance the efficiency of solar cells [27,28] and biological activities [29].

* Corresponding author.
E-mail address: ashok_sidarai@rediffmail.com (A.H. Sidarai).

http://dx.doi.org/10.1016/j.jphotochem.2017.06.003
1010-6030/

TiO_2 doping with rare earth material has been an effective method to enhance the photocatalytic activity because rare earth material having a special; electronic structure, which play an important role for the photo-generate charges transfer between 4f energy level and TiO_2 conduction band [30]. Doping of appropriate amount of La^{3+}, Ce^{3+}, Er^{3+}, Pr^{3+}, Gd^{3+}, Nd^{3+} and Sm^{3+} with TiO_2 can effectively enhance the photocatalytic activities, in further it is increased the adsorption capacity and also adsorption rate of TiO_2 catalysts. Here, it was found that gadolinium doping was most effective [31]. Zhou et al. reported that on doping gadolinium (Gd) with TiO_2 nanofibers their photocatalytic activity was enhanced [32]. Moreover, it is well known that half-filled electron configurations are more stable. Gd element has a half-filled 4f-shell containing only seven electrons and an empty 5d-shell, which are different from the other rare earth elements [33]. Therefore, the rare earth Gd^{3+} may serve as a superior co-catalyst for improving photocatalytic activity. According to the analysis, as discussed above, it can be deduced that Gd doping may be an ideal photocatalytic material with high photocatalytic activity.

The high degree of microbial diseases and their multidrug resistant properties make the researchers to develop a new class of antimicrobial agents [34–37]. A modern and innovative approach to drug development is the use of metallic NPs as new formulations of antimicrobial agents. Herein, the present study attempts to utilize the green route for the synthesis of gadolinium doped titanium dioxide (GdT) NPs for to study their optical, structural, morphology and thermal behaviors. Further, GdT NPs were tested for their antimicrobial and antioxidant activities. To the best of our knowledge, it is the first attempt to synthesize the Gd-doped TiO_2 NPs via hydrothermal method using *Piper betel* leaf extract as a capping and stabilizing agents also there are no reports on biological activities of GdT NPs.

2. Materials and methods

2.1. Chemicals

Titanium (IV) *n*-butoxide (TNB, $C_{16}H_{36}O_4Ti$) [99 Wt% liquid analytical grade] was purchased from Alfa Aesar chemicals and gadolinium (Gd) nitrate was purchased from Sigma-Aldrich chemical company. Ascorbic acid, ethanol and methanol were purchased from Spectrochem Laboratories Pvt. Ltd India and 1, 1-diphenyl-2-picrylhydrazyl (DPPH) was purchased from HiMedia Laboratories Pvt. Ltd. India and were used without any further purification. De-ionized water (DW) is used in the preparation of all suspensions and solutions. All glass wares were washed before use with dilute nitric acid and dried in an oven.

2.2. Biological materials

The leaves of *Piper betel* were purchased from local market Dharwad, Karnataka, India. Antimicrobial activities were tested using *Staphylococcus aureus* as a Gram-positive bacterium, *Escherichia coli* as a Gram-negative bacterium and *Candida albicans* as a fungus organism.

2.3. Preparation of leaf extract

20 g of chopped *Piper betel* leaves were added into 250 ml Erlenmeyer flask along with 100 ml of DW and later stirred using a magnetic heating stirrer at 80 °C for 30 min. The obtained supernatant solution was filtered with the Whatman filter paper No. 1, stored below 20 °C and used within a week.

2.4. Green synthesis of GdT NPs

GdT NPs were synthesized according to a method described in previous report [23], with little modifications. Briefly, 0.1 M of gadolinium nitrate was taken in 10 ml of DW in 25 ml beaker, stirred for 10 min at room temperature. Then 5 ml of *Piper betel* leaf extract and 1 ml of TNB were added to that mixture and stirred for 30 min, it turns to the brown color solution from transparent solution. The brown colloidal solution was then transferred to a 25 ml Teflon-lined stainless steel autoclave, the autoclave was sealed and placed in an oven and heated upto 180 °C for 3 h, then the autoclave was cool down to room temperature. Under the ambient conditions, the reaction mixture was centrifuged to collect the product; the product was washed continuously with DW and ethanol. The final product was dried in an oven at 50 °C for 1 h. The obtained product is in powder form and it was used for various characterizations. Further, it is used for the biological activities.

2.5. Instrumentations and characterizations

UV–vis spectrophotometer (Model- V-670 JASCO at USIC, K. U. Dharwad, India) was used to record the absorption spectrum. Fourier transform infrared spectroscopy (FT-IR) (Model- Nicolet 6700 at USIC, K. U. Dharwad, India) was used for to analyze the absorption bands. X-ray diffraction (XRD) (Model- Bruker AXS D8 Advance at STIC, Cochin, India) analysis was carried out for the crystal structure and grain size estimation. Transmission electron microscopy (TEM) (Model- JEOL/JEM- 2100 at STIC, Cochin, India) and scanning electron microscopy (SEM) (Model- JEOL/JSM-6390LV at STIC, Cochin, India) analysis were examined for the

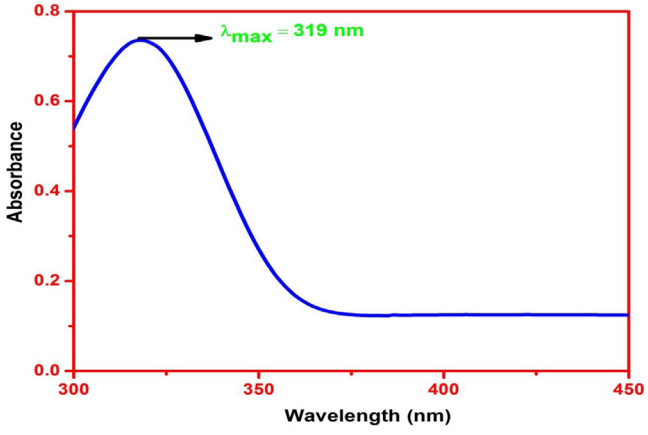

Fig. 1. UV–vis absorption spectrum of GdT NPs.

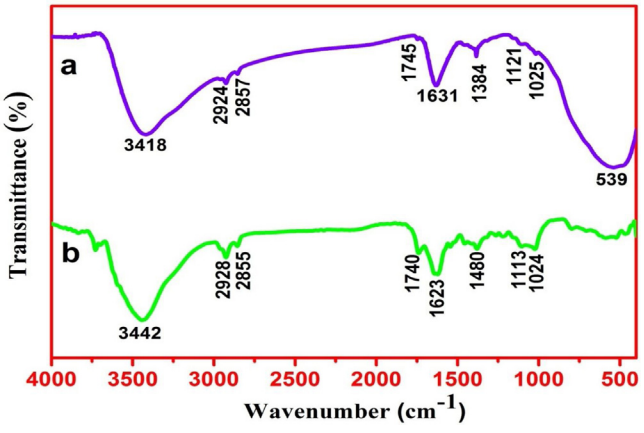

Fig. 2. FT-IR spectra **(a)** GdT NPs and **(b)** *Piper betel* leaf.

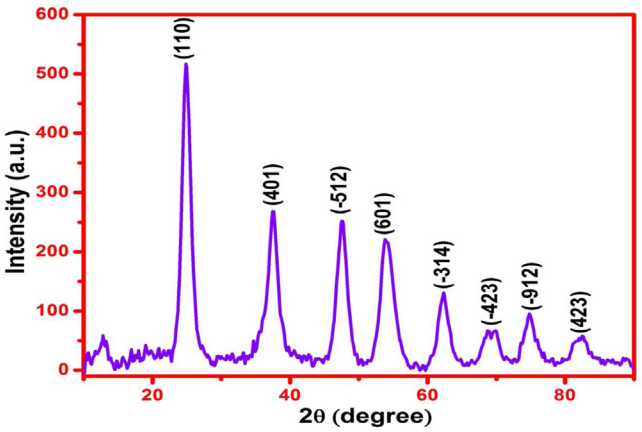

Fig. 3. XRD pattern for GdT NPs.

surface morphology and size distribution. Energy dispersive X-ray spectroscopy (EDS) (Model- NORAN system 7 at University of Mysore, Mysuru, India) was analyzed for the elemental compositions. Thermo gravimetric analysis (TGA) (Model- SDT Q600 at USIC, K. U. Dharwad, India) was used for measurement of thermal decompositions.

2.6. Antimicrobial assays

An antimicrobial susceptibility was tested using the agar-well diffusion method as described by G. Rajakumar et al. [26] for two different conditions i.e.,

1. UV irradiated sample
2. Without UV irradiated sample

Briefly, Lag phase cultures of *S. aureus*, *E. coli* and *C. albicans* were used as the test microorganisms. 100 μl of the standardized cell suspensions were spread on a Mueller-Hinton agar (Hi-Media) and the agar medium was punched with four wells having 6 mm diameter and filled with four different concentrations (25, 50, 75 and 100 μg mL^{-1} in DW) of GdT NPs into the respective wells. Then these Petri plates were incubated at 37 °C for 24 h in the incubator during which the activity was evidenced by the presence of a zone of inhibition surrounding the wells and it was measured in millimeters. In the case of *C. albicans*, Mueller-Hinton agar was replaced by Potato dextrose agar medium was used but here the plates were incubated at 27 °C for 48 h.

For the UV irradiated condition the powder samples were pre-irradiated for 12 h using 365 nm UV light source at a distance of 10 cm from the sample, then immediately various concentration of samples (taken in a DW) were added to the respective wells and kept at 4 °C for 20 min for the pre-diffusion. Later, these Petri plates were incubated at 37 °C for 24 h in an incubator.

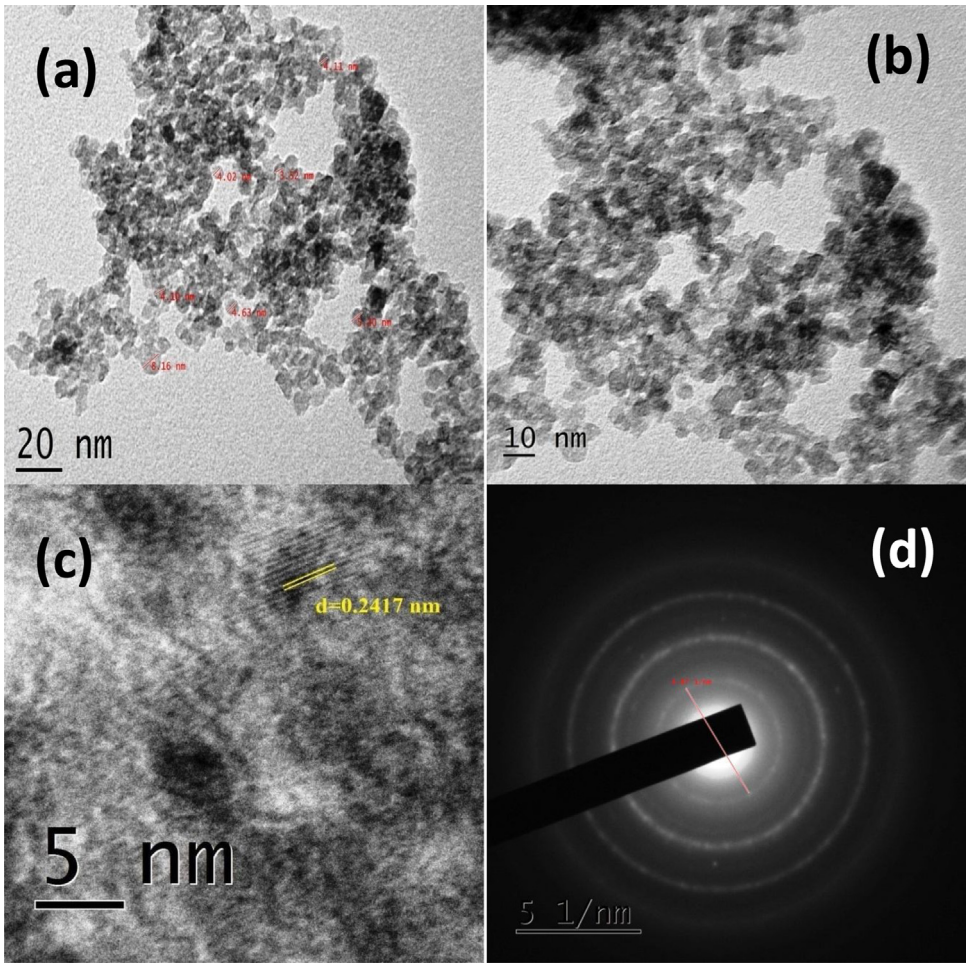

Fig. 4. TEM images for GdT NPs **(a)** 20 nm magnification, **(b)** 10 nm magnification, **(c)** 5 nm magnification and **(d)** SAED pattern.

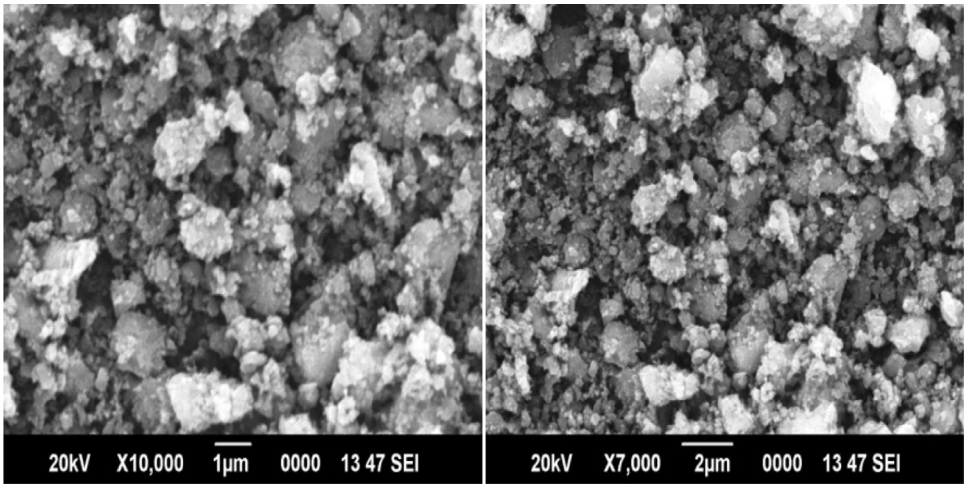

Fig. 5. SEM images of GdT NPs.

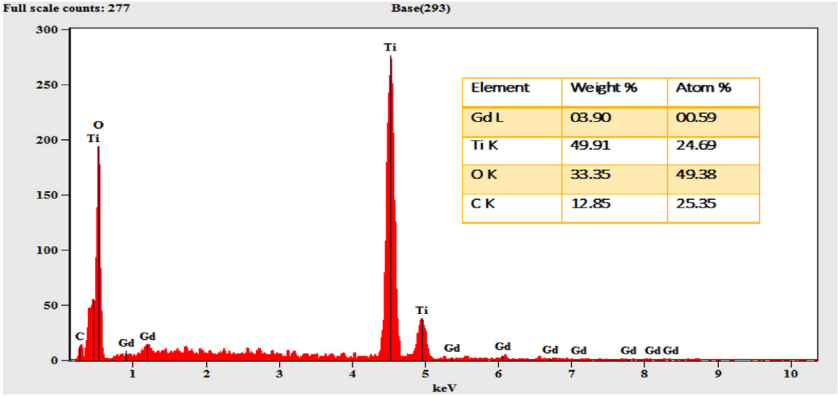

Fig. 6. EDS spectrum of GdT NPs with inset corresponding weight % and atomic % of elements.

For without UV irradiated condition the various concentrations of sample were directly added into the respective wells without illuminating UV radiation and kept for pre-diffusion process then placed in an incubator.

2.7. Antioxidant assays

An antioxidant activities of the GdT NPs and *Piper betel* leaf extract were measured on the basis of the free radical scavenging activity using the DPPH method [38]. The stock solution of DPPH was prepared by dissolving 3.9432 mg of DPPH in 100 ml of methanol and stored at 4 °C until use. 2 ml of DPPH solution was mixed with 1 ml of five different concentrations (20, 40, 60, 80 and 100 μg mL^{-1}) of the GdT NPs and *Piper betel* leaf extract. Ascorbic acid (20, 40, 60, 80 and 100 μg mL^{-1}) was used as a standard reference. A mixture of 1 ml of distilled water and 2 ml of DPPH solution was used as the control. The reaction mixture was mixed in the dark for 30 min and incubated at room temperature. The absorbance was recorded spectrophotometrically at 517 nm. An antioxidant activity was estimated based on the percentage of DPPH radical scavenged as the following equation

$$\text{Scavenging effect } \% = \frac{[\text{control absorbance} - \text{sample absorbance}]}{\text{control absorbance}} \times 100 \quad (1)$$

2.7.1. Statistical analysis

Statistical analysis was carried out using the SPSS software, version 20.0. Experiments were carried out in triplicates and the data was expressed as mean ± standard deviation by the One-Way ANOVA test. The Turkey's multiple comparison tests were used to determine significant differences between the standard and synthesized NPs. Correlation analysis was carried out using the Pearson's correlation analysis with $p = 0.01$. The linear regression analysis was carried out using the ORIGIN-8 software.

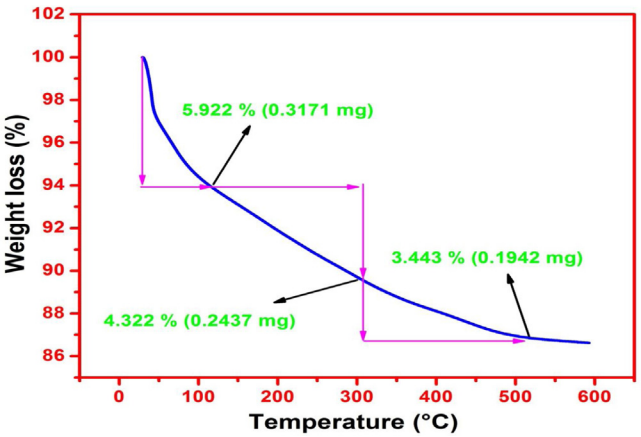

Fig. 7. TGA curve for GdT NPs.

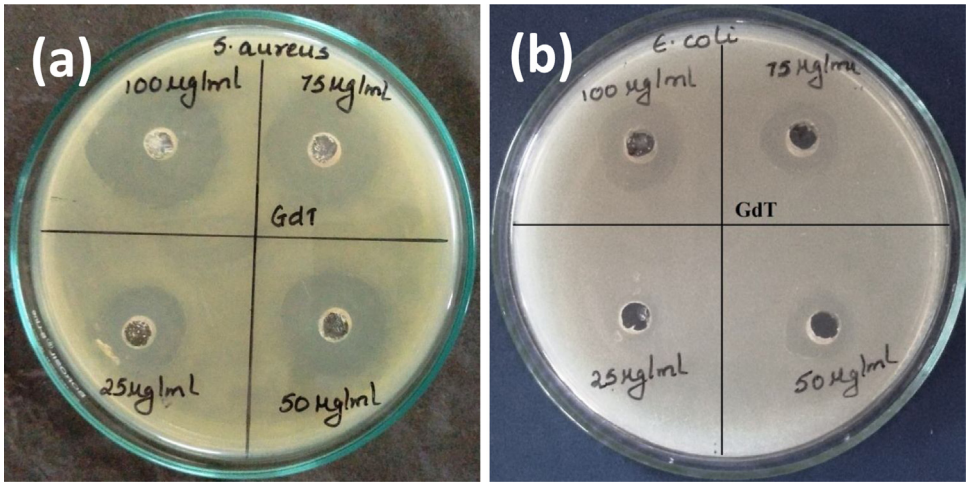

Fig. 8. Antibacterial activities of GdT NPs in UV irradiated condition **(a)** *S. aureus* and **(b)** *E. coli*.

3. Results and discussion

3.1. Optical properties

UV-vis spectroscopy analysis is an effective method to investigate whether the precursors are completely reduced or not. Here, the UV–vis absorption spectrum of GdT NPs was recorded in an optical range from 200 to 600 nm in ethanol solvent for 1×10^{-4} M concentration at room temperature. Fig. 1 represents the UV–vis spectrum of GdT NPs. From Fig. 1 it is observed that the absorption maximum (λ_{max}) is at 319 nm, which is a preliminary indication for the presence of TiO_2 and Gd materials [31]. In our previous publication for the green synthesized bare TiO_2 NPs, we observed the λ_{max} value is at 342 nm [23]. As compared with the previous report, TiO_2 NPs absorb light at much longer wavelength than Gd doped TiO_2. In other words, the decrease of particle size in Gd doped TiO_2 NPs might be the cause for the shift of onset of absorbance towards shorter wavelength. Due to this, the absorption maximum of Gd-doped TiO_2 NPs was hypsochromic shifted (lower wavelength).

3.2. Functional groups analysis

FT-IR spectroscopy was carried out to analyze the presence of functional groups which are responsible for the reduction of GdT NPs. FT-IR spectra of the samples were recorded in the range of 4000 to 400 cm^{-1} at a resolution of 2 cm^{-1} in the KBr pelletization method. Fig. 2 **(a** and **b)** represent the FT-IR spectra of GdT NPs and *Piper betel* leaf respectively. The FT-IR absorption peaks were analyzed according to N. B. Colthup [39] and J. Coates [40]. From Fig. 2 **(b)** it is revealed that the peak at 3442 cm^{-1} corresponds to free N—H stretching (aliphatic) it indicates the presence of amine groups, 2928 and 2855 cm^{-1} are correspond to methyl C—H asymmetric and symmetric stretching respectively, it may indicate that the presence of proteins and lipids, 1740 cm^{-1} corresponds to C=O stretching within the cage of cyclic peptides, 1623 and 1480 cm^{-1} are correspond to N—H asymmetric (amide I) and symmetric (amide II) bending, these absorption bands were arising corresponds to carbonyl stretch in proteins, the peak at 1113 cm^{-1} corresponds to O—H bending (water molecules) and the peak 1024 cm^{-1} corresponds to C—O stretching (secondary alcohol) [40]. Fig. 2 **(a)** shows a strong peak at 539 cm^{-1} is attributed to characteristic vibrational modes of Ti-O and Gd-O [41], from the observed absorption peaks in Fig. 2 **(b)** were some of the peaks are present and absent in Fig. 2 **(a)**. In Fig. 2 **(a)** the peak at 3418 cm^{-1} (free N—H stretching) is broadening due to the formation of H-bonds between amide groups, which will break the most of the H-bonds between the N—H groups and lead to bathochromic shift (higher to lower wave number). The peaks at 2924 and 2857 cm^{-1} correspond to the methyl C—H asymmetric and symmetric stretching respectively [40]. Some pronounced peaks from 1025 to 1745 cm^{-1} were observed and they have a hypsochromic shift (lower to higher wavenumber). The main difference between the spectra of Fig. 2 **(a)** and Fig. 2 **(b)** is the proper alteration of various peaks; this phenomenon indicates that biomolecules in *Piper betel* leaf, such as alkaloids, phenols, flavonoids, amino acids, glycosides and tannins are responsible for biotransformation of GdT ions to GdT NPs.

3.3. Crystallographic structure

XRD was analyzed to investigate the crystallographic structure and grain size of GdT NPs. XRD pattern was recorded at a scanning rate of 0.02 ° per second in the range of 20 ° to 80 ° using the Cu Kα radiation (Wavelength = 1.54060 Å). Fig. 3 shows the XRD pattern for GdT NPs. Here, it observed that there are sharp, broad and strong peaks; it may indicate the formation of the well-crystallized

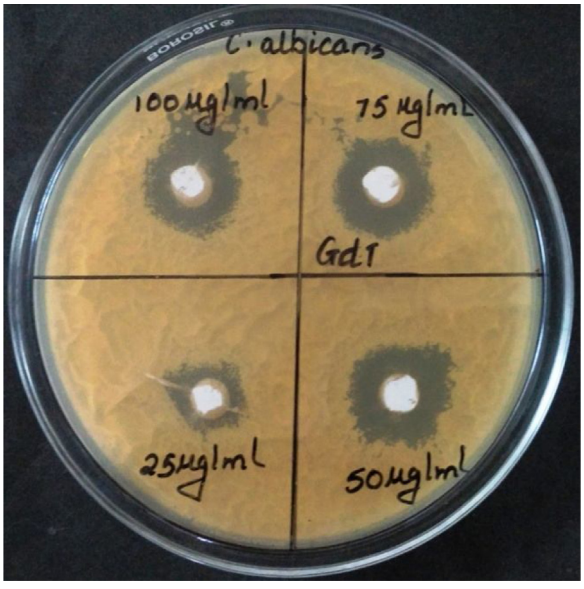

Fig. 9. Antifungal activity of GdT NPs in UV irradiated condition with *C. albicans*.

Table 1
Antimicrobial activity of GdT NPs in UV irradiated sample and without UV irradiated sample.

Material	Concentration ($\mu g\,mL^{-1}$)	Zone of inhibition (mm)					
		S. aureus		*E. coli*		*C. albicans*	
		Without UV	*With UV*	*Without UV*	*With UV*	*Without UV*	*With UV*
GdT NPs	25	10	15	10	11	12	13
	50	12	17	11	13	14	16
	75	14	19	12	14	15	18
	100	17	22	13	16	16	20

sample. Herein, we observed that the Bragg's reflection peaks at 2θ; 24.91°, 37.64°, 47.63°, 53.39°, 62.37°, 68.82°, 74.87° and 82.48° and their corresponding reflection planes are (110), (401), (−512), (601), (−314), (−423), (−912) and (423) respectively were obtained by comparing with the JCPDS data No. 46-1238, which may reveal that the material is having rutile phase with the monoclinic crystal structure. No any further reflection peaks for Gd can be noticed. The grain size of GdT NPs was calculated using the Scherrer's equation [42] for the most intense peak (110) and the calculated grain size is found to be 5.45 nm.

3.4. Morphology, size distribution and elemental analysis

TEM and SEM were examined to analyze the surface morphology and distribution of the size for the GdT NPs. Fig. 4 **(a, b** and **c)** show the typical TEM images and Fig. 4 **(d)** shows the SAED pattern for the GdT NPs. The observed GdT NPs are a uniform sphere in morphology with a diameter ranging from 4 nm to 7 nm. Agglomeration of the GdT NPs was observed due to the non-dispersion of the particles in a solvent before the sample preparation for TEM. On the other hand, a diffused rings and a bright spot in the SAED pattern indicate that the sample is well crystallized in nature. Fig. 5 represents the SEM images for GdT NPs, these images indicate that the particles are having a spherical cluster with an average size of about 40 nm to 60 nm. EDS was examined for to investigate the chemical compositions in GdT NPs. Fig. 6 represents the EDS spectrum for GdT NPs, from EDS spectrum it is confirmed that there is the presence of elements Gd, Ti and O. In addition, small quantities of element C is present, which is a residue of phytochemicals. The weight percentage (%) and atomic weight percentage (%) of GdT NPs are shown inset of Fig. 6.

3.5. Thermal properties

In view of identifying the thermal stability of GdT NPs; TGA study was carried out. For TGA, about 5 mg of GdT NPs was placed in a pan and heated from room temperature (28 °C) – 600 °C with a heating rate of 10 °C min^{-1} under nitrogen atmosphere. Fig. 7 shows the TGA curve for GdT NPs. From the TGA curve, it is observed that there are thermal decompositions occurs between 28 ° C - 600 °C. Initially, from 28 to 117 °C the GdT NPs are attributed the weight loss of about 5.922 % (0.3171 mg) it may be due to the desorption of physically absorbed water molecules, then from 117 to 306 °C is about 4.322 % (0.2437 mg) and from 306 to 516 °C about 3.443 % (0.1942 mg) may be due to the removal of chemically absorbed water molecule and phytochemicals [43,44]. Above 500 °C the material is in quite stable up to 600° C.

3.6. Antimicrobial assessments

Antimicrobial activities were evaluated against the two human pathogenic bacteria and a fungus, namely *S. aureus, E. coli* and *C. albicans* using the agar well diffusion method for two different conditions

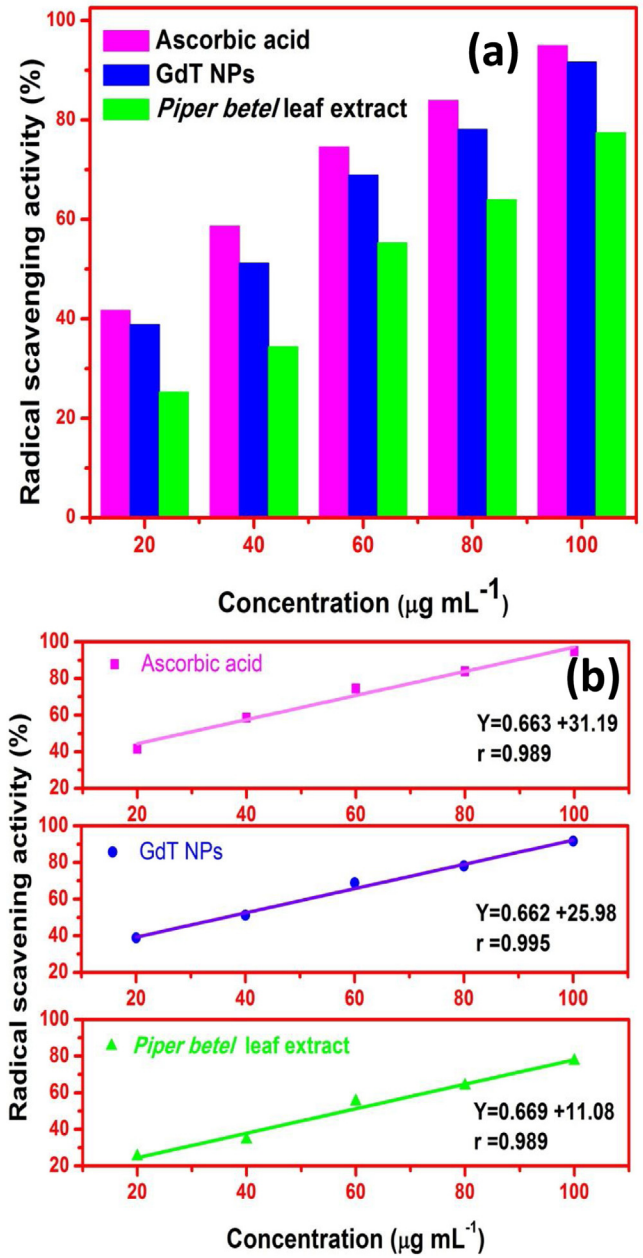

Fig. 10. **(a)** Radical scavenging activities of ascorbic acid, GdT NPs and *Piper betel* leaf extract **(b)** Linear correlation between concentrations and radical scavenging activities of ascorbic acid, GdT NPs and *Piper betel* leaf extract.

Table 2
DPPH free radical scavenging activities of standard ascorbic acid, GdT NPs and *Piper betel* leaf extract for five different concentrations along with their corresponding IC_{50} value and correlation coefficient (r).

Material	Concentration ($\mu g\,mL^{-1}$)	Radical scavenging activity (%)[a]	IC_{50} ($\mu g\,mL^{-1}$)	Correlation coefficient
Standard ascorbic acid	20	41.680 ± 1.064	23.99	0.989
	40	58.620 ± 1.066		
	60	74.546 ± 2.261		
	80	83.902 ± 1.402		
	100	94.946 ± 1.360		
GdT NPs	20	38.836 ± 0.965	25.74	0.995
	40	51.215 ± 1.435		
	60	68.893 ± 1.260		
	80	78.135 ± 1.643		
	100	91.650 ± 1.513		
Piper betel leaf extract	20	25.252 ± 0.988	58.14	0.989
	40	34.396 ± 1.047		
	60	55.266 ± 1.763		
	80	63.963 ± 1.570		
	100	77.430 ± 2.196		

Values are expressed as mean ± SD of n = 3 in each group.
[a] Correlation is significant at the 0.01 level.

1. UV irradiated sample
2. Without UV irradiated sample

Fig. 8 **(a** and **b)** show antibacterial activities of GdT NPs with *S. aureus* and *E. coli* for UV irradiated condition. Fig. 9 shows an antifungal activity of GdT NPs with *C. albicans* for UV irradiated condition. From Fig. 8 **(a** and **b)** it is observed that GdT NPs was an exhibit excellent antibacterial activity with the zone of inhibition on the culture plates. The zone of inhibition measurements were measured in millimeter for four different concentrations (25, 50, 75 and 100 $\mu g\,mL^{-1}$) at two different conditions and are tabulated in Table 1. From Table 1 it is observed that UV irradiated GdT NPs show a more zone of inhibition for all four different concentrations as compared to without UV irradiated samples. Further, it may infer that GdT NPs show comparatively higher antibacterial activity for *S. aureus* as compared to *E. coli*. The MIC value for GdT NPs is 25 $\mu g\,mL^{-1}$ for both the conditions. In the earlier case, we reported that the antibacterial activities for green synthesized TiO_2 NPs show comparatively less zone of inhibition against *S. aureus* and *E. coli*, but while doping TiO_2 with Gd the tested antimicrobial activity was enhanced.

In general, photocatalytic activity was enhanced due to the Gd ions do not enter the matrix of TiO_2, which are uniformly adsorbed on the surface of TiO_2. This is because the radius of Gd^{3+} (93.8 pm) is much larger than that of Ti^{4+} (68 pm) [45]. Thus, the dopant acts as a trapper to capture the photo-generated electrons, which is helpful for efficiently separating charge carriers, prolonging the life of the carriers, inhibiting the recombination of electron-hole pairs and resulting in the enhancement of the reactivity. Additionally, Gd has a half-filled electron configuration thus it is very stable. If Gd has captured an electron then the electron configuration will be destroyed. But trapped electrons can be transferred to adsorbed oxygen species and hydroxyl ions on the surface and in this way, stable electron configuration is recovered [31–33]. This procedure may lead to the formation of the hydroxyl radicals and oxygen radicals. These reactive oxygen species (ROS) generated on the surface of TiO_2 NPs are responsible for oxidative damage of cell membrane. The substantial enhancement of GdT NPs was attributed to the bandgap, high surface area and high surface hydroxylation group [46–48]. It is well known that surface hydroxyl groups play an important role in the photocatalytic activities [49,50].

3.7. Antioxidant assessments

Antioxidant activities of GdT NPs and *Piper Betel* leaf extract were studied using the DPPH method. Ascorbic acid was taken as a standard reference. Here, we have taken five different concentrations (20, 40, 60, 80 and 100 $\mu g\,mL^{-1}$) of ascorbic acid, GdT NPs and *Piper betel* leaf extract. After accepting a hydrogen radical from ascorbic acid, GdT NPs and *Piper betel* leaf extract, the DPPH was converted into the stable DPPH-H complex then the color of the solution will change from deep violet to light yellow. The percentage of scavenging activity was calculated using an equation (1). Radical scavenging activities of ascorbic acid, GdT NPs and *Piper betel* leaf extract are as shown in Fig. 10 **(a)**. The Linear correlation between concentration and radical scavenging activities of ascorbic acid, GdT NPs and *Piper betel* leaf extract are shown in Fig. 10 **(b)**. From Fig. 10 **(b),** we observed the good correlation value in all three cases. Table 2 shows the radical scavenging activities of ascorbic acid, GdT NPs and *Piper betel* leaf of five different concentrations along with their corresponding values of IC_{50} and correlation coefficient respectively. From Table 2, we observed that radical scavenging activity tends to increase with increasing the concentrations of antioxidant materials. Here, for all the five concentrations of ascorbic acid shows scavenging rate ranging from 41 to 95 %, GdT NPs show 39 – 92 % and for *Piper betel* leaf extract shows 25–77 %. Comparatively, ascorbic acid has the highest radical scavenging activity with the lowest IC_{50} value 23.99 $\mu g\,mL^{-1}$, GdT NPs show moderate IC_{50} value 25.74 $\mu g\,mL^{-1}$ and *Piper betel* leaf extract has the lowest radical scavenging activity with the highest IC_{50} value 58.14 $\mu g\,mL^{-1}$.

4. Conclusion

This work demonstrates the potential of gadolinium doped titanium dioxide (GdT) nanoparticles (NPs) on the biological activities. Herein, we green synthesized the GdT NPs via hydrothermal method using the *Piper betel* leaf as capping and reducing agents. GdT NPs were subjected to various characterizations for their optical, structural, functional group, surface morphology, elemental analysis and thermal studies. Results suggest that they are having crystalline in nature and spherical shape with a size of about 4–7 nm. GdT NPs are thermally quite stable from room temperature to 500 °C with the weight loss of

about 14 %. Further, these GdT NPs show potent antimicrobial agent for the microorganisms *(S. aureus*, *E. coli* and *C. albicans)* and also they possess excellent antioxidant activities. Moreover, we believe that this work could pave the way for nano-sized drug delivery applications for the treatment of several diseases.

Acknowledgements

The authors (Shirajahammad and Vani) acknowledge the financial support under the UGC-UPE fellowship from Karnatak University Dharwad (KU/SCH/UGC-UPE/2014-15/915 and KU/SCH/UGC-UPE/2014-15/916). Authors are thankful to the technical staff of USIC, Karnatak University Dharwad for UV–vis, FT-IR and TGA measurements.

References

[1] H. Duan, D. Wang, Y. Li, Green chemistry for nanoparticle synthesis, Chem. Soc. Rev. 44 (2015) 5778–5792, doi:http://dx.doi.org/10.1039/c4cs00363b.
[2] C.A. Mirkin, T.A. Taton, Semiconductors meet biology, Nature 405 (2000) 626–627, doi:http://dx.doi.org/10.1038/35015190.
[3] M.C.M. Daniel, D. Astruc, Gold nanoparticles: assembly, supramolecular chemistry, quantum-Size-Related properties and applications toward biology, catalysis and nanotechnology, Chem. Rev. 104 (2004) 293–346, doi:http://dx.doi.org/10.1021/cr030698.
[4] M. Auffan, J. Rose, J.Y. Bottero, G.V. Lowry, J.P. Jolivet, M.R. Wiesner, Towards a definition of inorganic nanoparticles from an environmental, health and safety perspective, Nat. Nanotechnol. 4 (2009) 634–641, doi:http://dx.doi.org/10.1038/nnano.2009.242.
[5] P.K. Jain, X. Huang, I.H. El-Sayed, M.A. El-Sayed, Noble metals on the nanoscale: optical and photothermal properties and some applications in imaging, sensing, biology, and medicine, Acc. Chem. Res. 41 (2008) 1578–1586, doi:http://dx.doi.org/10.1021/ar7002804.
[6] S. Lee, I.S. Cho, J.H. Lee, D.H. Kim, D.W. Kim, J.Y. Kim, H. Shin, J.K. Lee, H.S. Jung, N.G. Park, K. Kim, M.J. Ko, K.S. Hong, Two-step sol-gel method-based TiO2 nanoparticles with uniform morphology and size for efficient photo-energy conversion devices, Chem. Mater. 22 (2010) 1958–1965, doi:http://dx.doi.org/10.1021/cm902842k.
[7] V. Caratto, F. Locardi, S. Alberti, S. Villa, E. Sanguineti, A. Martinelli, T. Balbi, L. Canesi, M. Ferretti, Different sol???gel preparations of iron-doped TiO2 nanoparticles: characterization, photocatalytic activity and cytotoxicity, J. Sol-Gel Sci. Technol. 80 (2016) 152–159, doi:http://dx.doi.org/10.1007/s10971-016-4057-5.
[8] S. Ashok Kumar, P.H. Lo, S.M. Chen, Electrochemical synthesis and characterization of TiO 2 nanoparticles and their use as a platform for flavin adenine dinucleotide immobilization and efficient electrocatalysis, Nanotechnology 19 (2008) 255501, doi:http://dx.doi.org/10.1088/0957-4484/19/25/255501.
[9] T. Arun, A.A. Madhavan, D.K. Chacko, G.S. Anjusree, T.G. Deepak, S. Thomas, S.V. Nair, A.S. Nair, A facile approach for high surface area electrospun TiO2 nanostructures for photovoltaic and photocatalytic applications, Dalton Trans. 43 (2014) 4830–4837, doi:http://dx.doi.org/10.1039/c3dt52780h.
[10] Z. Song, J. Hrbek, R. Osgood, Formation of TiO 2 nanoparticles by reactive-layer-assisted deposition and characterization by XPS and STM, Nano Lett. 5 (2005) 1327–1332, doi:http://dx.doi.org/10.1021/nl0505703.
[11] D. Reyes-Coronado, G. Rodríguez-Gattorno, M.E. Espinosa-Pesqueira, C. Cab, R. de Coss, G. Oskam, Phase-pure TiO(2) nanoparticles: anatase, brookite and rutile, Nanotechnology 19 (2008) 145605, doi:http://dx.doi.org/10.1088/0957-4484/19/14/145605.
[12] S.S. Mali, C.A. Betty, P.N. Bhosale, Pramod S. Patil, CrystEngComm Hydrothermal synthesis of rutile TiO 2 with hierarchical microspheres and their characterization, CrystEngComm 13 (2011) 6349–6351, doi:http://dx.doi.org/10.1039/c1ce05928a.
[13] S. Ahmed, M. Ahmad, B.L. Swami, S. Ikram, A review on plants extract mediated synthesis of silver nanoparticles for antimicrobial applications: a green expertise, J. Adv. Res. 7 (2016) 17–28, doi:http://dx.doi.org/10.1016/j.jare.2015.02.007.
[14] N. Ahmad, S. Sharma, M.K. Alam, V.N. Singh, S.F. Shamsi, B.R. Mehta, A. Fatma, Rapid synthesis of silver nanoparticles using dried medicinal plant of basil, Colloids Surf. B Biointerfaces 81 (2010) 81–86, doi:http://dx.doi.org/10.1016/j.colsurfb.2010.06.029.
[15] R. Geethalakshmi, D.V.L. Sarada, Synthesis of plant-mediated silver nanoparticles using Trianthema decandra extract and evaluation of their anti microbial activities, Int. J. Eng. Sci. Technol. 2 (2010) 970–975, doi:http://dx.doi.org/10.1155/2011/573429.
[16] A. Weir, P. Westerhoff, L. Fabricius, N. von Goetz, Titanium dioxide nanoparticles in food and personal care products, Environ. Sci. Technol. 46 (2012) 2242–2250, doi:http://dx.doi.org/10.1021/es204168d.
[17] R.A. French, A.R. Jacobson, B. Kim, S.L. Isley, R.L.E.E. Penn, P.C. Baveye, Influence of ionic strength, pH, and cation valence on aggregation kinetics of titanium dioxide nanoparticles, Environ. Sci. Technol. 43 (2009) 1354–1359, doi:http://dx.doi.org/10.1021/es802628n.
[18] A. Kay, M. Grätzel, Low-cost photovoltaic modules based on dye sensitized nanocrystalline titanium dioxide and carbon powder, Sol. Energy Mater. Sol. Cells. 44 (1996) 99–117, doi:http://dx.doi.org/10.1016/0927-0248(96)00063-3.
[19] J. Bai, B. Zhou, Titanium dioxide nanomaterials for sensor applications, Chem. Rev. 114 (2014) 10131–10176, doi:http://dx.doi.org/10.1021/cr400625j.
[20] Y. Shibata, T. Miyazaki, Biological activity of titanium, Handb. Oral Biomater. 97 (2014) 93–97, doi:http://dx.doi.org/10.4032/9789814463133.
[21] X. Chen, S.S. Mao, Titanium dioxide nanomaterials: synthesis, properties, modifications and applications, Chem. Rev. 107 (2007) 2891–2959, doi:http://dx.doi.org/10.1021/cr0500535.
[22] M. Atarod, M. Nasrollahzadeh, S. Mohammad Sajadi, Euphorbia heterophylla leaf extract mediated green synthesis of Ag/TiO2 nanocomposite and investigation of its excellent catalytic activity for reduction of variety of dyes in water, J. Colloid Interface Sci. 462 (2016) 272–279, doi:http://dx.doi.org/10.1016/j.jcis.2015.09.073.
[23] S.M. Hunagund, V.R. Desai, J.S. Kadadevarmath, D.A. Barretto, S. Vootla, A.H. Sidarai, Biogenic and chemogenic synthesis of TiO2 NPs via hydrothermal route and their antibacterial activities, RSC Adv. 6 (2016) 97438–97444, doi:http://dx.doi.org/10.1039/C6RA22163G.
[24] S.M. Roopan, A. Bharathi, A. Prabhakarn, A. Abdul Rahuman, K. Velayutham, G. Rajakumar, R.D. Padmaja, M. Lekshmi, G. Madhumitha, Efficient phyto-synthesis and structural characterization of rutile TiO2 nanoparticles using Annona squamosa peel extract, Spectrochim. Acta – Part A Mol. Biomol. Spectrosc. 98 (2012) 86–90, doi:http://dx.doi.org/10.1016/j.saa.2012.08.055.
[25] M. Nasrollahzadeh, S.M. Sajadi, Synthesis and characterization of titanium dioxide nanoparticles using Euphorbia heteradena Jaub root extract and evaluation of their stability, Ceram. Int. 41 (2015) 14435–14439, doi:http://dx.doi.org/10.1016/j.ceramint.2015.07.079.
[26] G. Rajakumar, A.A. Rahuman, S.M. Roopan, V.G. Khanna, G. Elango, C. Kamaraj, A.A. Zahir, K. Velayutham, Fungus-mediated biosynthesis and characterization of TiO 2 nanoparticles and their activity against pathogenic bacteria, Spectrochim. Acta – Part A Mol. Biomol. Spectrosc. 91 (2012) 23–29, doi:http://dx.doi.org/10.1016/j.saa.2012.01.011.
[27] J. Reszczyńska, T. Grzyb, J.W. Sobczak, W. Lisowski, M. Gazda, B. Ohtani, A. Zaleska, Visible light activity of rare earth metal doped (Er3+, Yb3+ or Er3+/Yb3+) titania photocatalysts, Appl. Catal. B Environ. 163 (2015) 40–49, doi:http://dx.doi.org/10.1016/j.apcatb.2014.07.010.
[28] S.M. Hunagund, P. Chavan, V.R. Desai, L.R. Naik, J.S. Kadadevarmath, A.H. Sidarai, Influence of Fe3+ ion substitution on thermal and dielectric properties of titanium dioxide, Int. Lett. Chem. Phys. Astron. 67 (2016) 9–13, doi:http://dx.doi.org/10.18052/www.scipress.com/ILCPA.67.9.
[29] A. García, L. Delgado, J.A. Torà, E. Casals, E. González, V. Puntes, X. Font, J. Carrera, A. Sánchez, Effect of cerium dioxide, titanium dioxide, silver, and gold nanoparticles on the activity of microbial communities intended in wastewater treatment, J. Hazard. Mater. 199–200 (2012) 64–72, doi:http://dx.doi.org/10.1016/j.jhazmat.2011.10.057.
[30] S. Bingham, W.A. Daoud, Recent advances in making nano-sized TiO 2 visible-light active through rare-earth metal doping, J. Mater. Chem. (2011) 2041–2050, doi:http://dx.doi.org/10.1039/c0jm02271c.
[31] M. Mahalakshmi, B. Arabindoo, M. Palanichamy, V. Murugesan, Preparation, characterization, and photocatalytic activity of Gd 3 + Doped TiO 2 nanoparticles, J. Nanosci. Nanotechnol. 7 (2007) 3277–3285, doi:http://dx.doi.org/10.1166/jnn.2007.689.
[32] S. Z.H.A.N.G, Z.H.U.S. Zhi-ping, L.I.Y. Tjct, ;1 Preparation and photocatalytic activity of Gd-doped TiO nanofibre, J. Cent. South Univ. Technol. 12 (2010) 657–661.
[33] W.Y. Zhou, Q.Y. Cao, Y.J. Liu, X.Y. Yu, Y. Luo, Enhancement of TiO 2 photocatalytic activity by Gd 3 doping, Adv. Appl. Ceram. 106 (2007) 222–226, doi:http://dx.doi.org/10.1179/17436760X62028.
[34] R. Singh, J.W. Lillard, Nanoparticle-based targeted drug delivery, Exp. Mol. Pathol. 86 (2009) 215–223, doi:http://dx.doi.org/10.1016/j.yexmp.2008.12.004.
[35] X. Li, S.M. Robinson, A. Gupta, K. Saha, Z. Jiang, D.F. Moyano, A. Sahar, M.A. Riley, V.M. Rotello, Functional gold nanoparticles as potent antimicrobial agents against multi-drug-resistant bacteria, ACS Nano. 8 (2014) 10682–10686, doi:http://dx.doi.org/10.1021/nn5042625.
[36] C.M.J. Hu, S. Aryal, L. Zhang, Nanoparticle-assisted combination therapies for effective cancer treatment, Ther. Deliv. 1 (2010) 323–334, doi:http://dx.doi.org/10.4155/tde.10.13.
[37] A.N. Brown, K. Smith, T.A. Samuels, J. Lu, S.O. Obare, M.E. Scott, Nanoparticles functionalized with ampicillin destroy multiple-antibiotic-resistant isolates of Pseudomonas aeruginosa and Enterobacter aerogenes and methicillin-resistant Staphylococcus aureus, Appl. Environ. Microbiol. 78 (2012) 2768––2774, doi:http://dx.doi.org/10.1128/AEM.06513-11.
[38] S. Zhao, M. Lan, X. Zhu, H. Xue, T. Ng, X. Meng, C. Lee, P. Wang, W. Zhang, Green synthesis of bifunctional fluorescent carbon dots from garlic for cellular imaging and free radical scavenging, ACS Appl. Mater. Interfaces. 7 (2015) 17054–17060, doi:http://dx.doi.org/10.1021/acsami.5b03228.
[39] N.B. Colthup, Spectra-Structure correlations in the infra-red region, J. Opt. Soc. Am. 40 (1950) 397, doi:http://dx.doi.org/10.1364/JOSA.40.000397.
[40] J. Coates, Interpretation of infrared spectra, a practical approach interpretation of infrared spectra, a practical approach, Encycl. Anal. Chem. (2000) 10815–10837, doi:http://dx.doi.org/10.1002/9780470027318.

[41] S. Liufu, H. Xiao, Y. Li, Adsorption of poly(acrylic acid) onto the surface of titanium dioxide and the colloidal stability of aqueous suspension, J. Colloid Interface Sci. 281 (2005) 155–163, doi:http://dx.doi.org/10.1016/j.jcis.2004.08.075.
[42] P.B. Patil, V.V. Kondalkar, N.B. Pawar, Single step hydrothermal synthesis of hierarchical TiO 2 micro fl owers with radially assembled nanorods for enhanced photovoltaic performance, RSC Adv. 4 (2014) 47278–47286, doi:http://dx.doi.org/10.1039/C4RA07682F.
[43] S. Jeon, P.V. Braun, Hydrothermal synthesis of Er-doped luminescent TiO 2 nanoparticles, Chem. Mater. (2003) 1256–1263, doi:http://dx.doi.org/10.1021/cm0207402.
[44] J. Wang, W. Sun, Z. Zhang, Z. Jiang, X. Wang, R. Xu, R. Li, X. Zhang, Preparation of Fe-doped mixed crystal TiO2 catalyst and investigation of its sonocatalytic activity during degradation of azo fuchsine under ultrasonic irradiation, J. Colloid Interface Sci. 320 (2008) 202–209, doi:http://dx.doi.org/10.1016/j.jcis.2007.12.013.
[45] D. Lu, P. Fang, Y. Liu, A facile one-pot synthesis of gadolinium doped TiO 2 −based nanosheets with efficient visible light-driven photocatalytic performance, J. Nanopart. Res. 16 (2014) 1–12, doi:http://dx.doi.org/10.1007/s11051-014-2636-3.
[46] A.R. Allafchian, S.Z. Mirahmadi-Zare, S.A.H. Jalali, S.S. Hashemi, M.R. Vahabi, Green synthesis of silver nanoparticles using phlomis leaf extract and investigation of their antibacterial activity, J. Nanostructure Chem. (2016), doi:http://dx.doi.org/10.1007/s40097-016-0187-0.
[47] M.J. Hajipour, K.M. Fromm, A. Akbar Ashkarran, D. Jimenez de Aberasturi, I.R. de Larramendi, T. Rojo, V. Serpooshan, W.J. Parak, M. Mahmoudi, Antibacterial properties of nanoparticles, Trends Biotechnol. 30 (2012) 499–511, doi:http://dx.doi.org/10.1016/j.tibtech.2012.06.004.
[48] K. Murugan, D. Dinesh, K. Kavithaa, M. Paulpandi, T. Ponraj, M.S. Alsalhi, S. Devanesan, J. Subramaniam, R. Rajaganesh, H. Wei, S. Kumar, M. Nicoletti, G. Benelli, Hydrothermal synthesis of titanium dioxide nanoparticles: mosquitocidal potential and anticancer activity on human breast cancer cells (MCF-7), Parasitol. Res. 115 (2016) 1085–1096, doi:http://dx.doi.org/10.1007/s00436-015-4838-8.
[49] S. Noimark, K. Page, J.C. Bear, C. Sotelo-Vazquez, R. Quesada-Cabrera, Y. Lu, E. Allan, J.A. Darr, I.P. Parkin, Functionalised gold and titania nanoparticles and surfaces for use as antimicrobial coatings, Faraday Discuss. 175 (2014) 273–287, doi:http://dx.doi.org/10.1039/c4fd00113c.
[50] E. Tridoped, T. Nanopowder, W. Wang, Q. Shang, W. Zheng, H. Yu, X. Feng, Z. Wang, Y. Zhang, G. Li, A Novel Near-Infrared Antibacterial Material Depending on the Upconverting Property of, (2010) , pp. 13663–13669.